

## 15.4

### Observations of severe storms by a low-power, polarimetric, phased array mobile radar

Robin L. Tanamachi\*, Allison T. LaFleur, Milind Sharma

*Purdue University, Department of Earth, Atmospheric, and Planetary Sciences (EAPS), West Lafayette, Indiana*

Stephen J. Frasier, William Heberling, Carl (Casey) Wolsieffer

*University of Massachusetts, Microwave Remote Sensing Laboratory (MIRSL), Amherst, Massachusetts*

#### 1. Introduction

The nationwide deployment by the U.S. National Weather Service of dual-polarized (DP) weather radar in the National Weather Service (NWS) operational WSR-88D network has brought about a new focus on polarimetric radar signatures attendant to severe weather hazards. At the same time, advantages to both research and operations conferred by rapid- but non-mechanically-scanning, single-polarized radars have been demonstrated convincingly (Heinselman et al. 2008; French et al. 2014; Wurman et al. 2014; Heinselman et al. 2015; Kurdzo et al. 2016). Since severe thunderstorms are rapidly evolving phenomena, they require commensurately rapid observation in order to effectively document internal dynamical and microphysical changes occurring on these short time scales (~30 s or less). For this reason, a great deal of effort and resources have been directed toward coupling DP and rapid scanning (RS) radar technology over the last decade. As an example, the rapidly scanning, X-band, polarimetric mobile Doppler radar (RaXPoI; Pazmany et al. 2013) has been used to great effect, capturing high temporal resolution observations of rapid evolution in severe storms and tornadoes (Bluestein et al. 2015; Houser et al. 2015; Houser et al. 2016). While RaXPoI is capable of collecting a full 360° sweep every 2 s with an azimuthal resolution of 1°, translation errors are introduced on even those short time scales by the need to rotate the antenna mechanically.

Phased array radar (PAR), which employs electronic beam formation and steering, holds the promise of much more rapid volumetric scanning ability than even a platform like RaXPoI can provide. Substantial engineering challenges remain, however, in coupling dual-polarization and phased array technology (Bluestein et al. 2014), ensuring orthogonality of polarized waves

off boresight. Nevertheless, examples abound of DP PARs in design and development (Zhang et al. 2010; Orzel 2015; Stailey and Hondl 2016; Salazar-Cerreño et al. 2017).

In this manuscript, we report on the deployment of a new, mobile, DP PAR for weather studies: The University of Massachusetts Low-Power Radar (UMass LPR; Heberling et al. 2019; this session) (Fig. 1; Table 1). The design of this radar, which was previously used for air traffic and weather applications, is a simplified version of that described by Puzella and Alm (2007). UMass LPR was mobilized in 2018 for severe weather research by the UMass Microwave Remote Sensing Laboratory (MIRSL) and fielded by students and faculty from Purdue University's Department of Earth, Atmospheric, and Planetary Sciences (EAPS).



**Fig. 1. EAPS students enrolled in the 2018 summer course “Severe Storms Field Work” practice deploying the UMass LPR at an agronomy research facility near Purdue campus.**

The purpose of the deployments was to collect high spatiotemporal resolution observations of differential reflectivity ( $Z_{DR}$ ) columns and arcs in potentially tornadic supercells. These features are hypothesized to have prognostic value for tornadogenesis on time

---

\* Corresponding author: Robin L. Tanamachi, Purdue University, Department of Earth, Atmospheric, and

Planetary Sciences, 550 West Stadium Avenue, West Lafayette, IN 47907. Email: [rtanamachi@purdue.edu](mailto:rtanamachi@purdue.edu)

scales of 1 to 5 minutes; therefore, RS DP radar observations are critical for updating conceptual models (Crowe et al. 2012; Picca et al. 2015).

Table 1. Selected parameters of the UMass LPR radar, as reported by Heberling et al. (2017).

Parameter	Value
Frequency	9.6 GHz
Peak/average transmitted power	125 W / 23 W
Half-power beam width	1.9° az., 2.1° el.
Polarization	Dual linear
Polarization scheme	ATAR
Maximum unambiguous range	40 km
Maximum unambiguous velocity (PRT1)	18.8 m s <sup>-1</sup>
Range resolution	60 m
Azimuthal sector	90°
Elevation angles	0° - 30° every 1°
Volume update time	~90 s
Antenna elements	2,580 (20 tiles x 128 elements)

## 2. 2018 field program

The Purdue-UMass field program operated out of West Lafayette, Indiana from 15 May to 30 June 2018. The field program was timed to align with a seasonal maximum in severe thunderstorm occurrence over the north central United States, which occurs slightly later than that in the southern Great Plains region. During this period, Purdue and UMass personnel forecast the potential for tornadic storms in a daily cycle, and targeted storms opportunistically for RS DP observations.

The field program partly coincided with the 2018 version of a Purdue EAPS summer course entitled “Severe Storms Field Work” (Tanamachi et al. 2019). In this course, a mixture of graduate and undergraduate students collected coordinated meteorological observations around severe storms using UMass LPR (e.g.; Fig. 1), a mobile radiosonde sounding system, and Portable In Situ Precipitation Sensor packages (Dawson et al. 2016). With the assistance of the students, the group successfully deployed UMass LPR near a supercell near Burwell, Nebraska on 1 June 2018. Those data will be exhibited in the next section.

After the summer course ended on 12 June, Purdue and UMass graduate students continued to opportunistically operate the UMass LPR without the other instruments, collecting data across multiple states (Fig. 2, Table 2). During these deployments, several Z<sub>DR</sub> columns and arcs were sampled at ~30 s temporal resolution. Some examples will be shown in the next section.

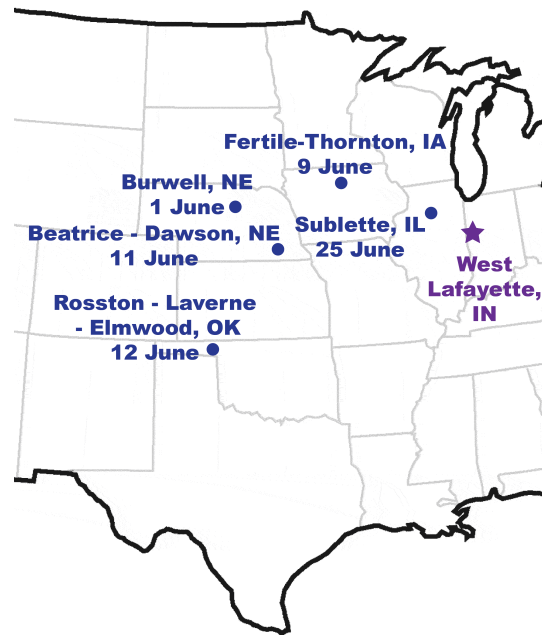


Fig. 2. Map of UMass LPR deployments in 2018 for storm observations (blue dots) relative to the location of West Lafayette, Indiana (purple star).

Table 2. Summary of UMass LPR deployments in severe storms during the 2018 field program. Additional test deployments are not shown.

Date	Location	Description
1 June	Burwell, NE	Supercell / Multicell cluster; wall cloud; <b>tornado genesis failure</b>
9 June	Fertile – Thornton, IA	Embedded supercell with possible tornado near Rockwell, IA (2128 UTC)
11 June	Beatrice - Dawson, NE	CI, MCS
12 June	Rosston – Laverne – Elmwood, OK	Slow-moving supercell on KS/OK border; <b>tornado genesis failure</b>
25 June	Sublette, IL	Interacting multicell storms

### 3. Examples of data

#### 3.1 1 June 2018: Supercell near Burwell, Nebraska

A cluster of interacting cells, some with transient mesocyclones, were observed in north central Nebraska on 1 June 2018 (local time). The severe storms field work class participants deployed UMass LPR about 11 km WNW of Burwell, Nebraska, targeting the southernmost cell in a line as it lifted northeastward. A wall cloud (not shown) was observed from the deployment site at 0045 UTC on 2 June. A well-defined hook echo (Fig. 3a) coincident with a Doppler velocity couplet (Fig. 3b) can be discerned at 0038 UTC on 2 June, just prior to the appearance of a wall cloud at 0045 UTC that was observed from the deployment site. A weak echo hole (not shown) was observed 2 min later at higher elevations, and likely represents an axial downdraft associated with the main mesocyclone (e.g., Tanamachi et al. 2012). No tornado was reported in this storm, although one was observed by members of the class later in the evening.

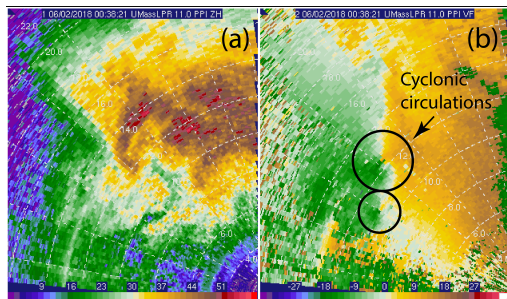


Fig. 3. UMass LPR (a) reflectivity (in dBZ) and aliased Doppler velocity (in  $\text{m s}^{-1}$ ) observed in the Burwell, Nebraska storm at 0038 UTC on 2 June 2018 at an elevation angle of  $11^\circ$ . Two cyclonic circulations (solid black circles) are annotated. Range rings (azimuth spokes) are drawn every 2 km ( $10^\circ$ ).

The  $Z_{\text{DR}}$  column is more meaningfully visualized in three dimensions (Fig. 4). To generate this visualization, the UMass LPR observations were objectively analyzed to a radar-centered Cartesian grid ( $\Delta x, \Delta y, \Delta z = 200$  m) using a single-pass Barnes objective analysis scheme. It can be seen that the UMass LPR did not sample the  $Z_{\text{DR}}$  column through its full depth because it was deployed at too short of a range (Fig. 4). At a range of  $\sim 12$  km, it appears that even the  $30^\circ$  scan does not top out the column. Therefore, we can only take the height of the  $Z_{\text{DR}}$

maximum in the  $30^\circ$  scan (5.3 km) as a lower bound on the actual  $Z_{\text{DR}}$  column height. Supercell  $Z_{\text{DR}}$  columns have previously been observed to extend as high as 8 km AGL (e.g., Snyder et al. 2015).

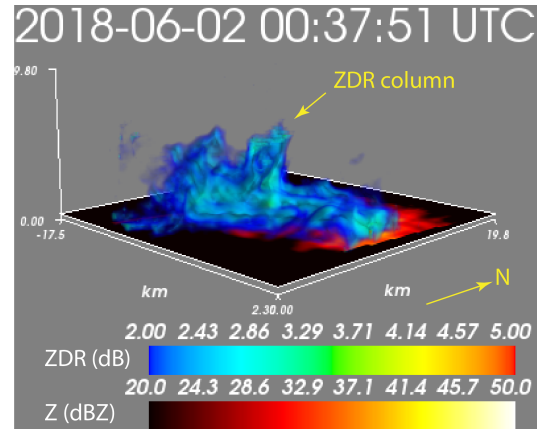


Fig. 4. Volume-rendered view of UMass LPR-measured  $Z_{\text{DR}}$  (cool colors, in dB) overlaid on a CAPPI of reflectivity (hot colors, in dBZ) at 200 m AGL for the volume collected at 0038 UTC on 2 June. The view is toward the northwest. The scalloped appearance of the top of the  $Z_{\text{DR}}$  column results from the objective analysis of the  $30^\circ$  scan onto the 200-m Cartesian grid.

The group observed a brief tornado near Ord, Nebraska at 0117 UTC on 2 June, but the UMass LPR was out of position to collect data owing to intervening terrain.

#### 3.2 12 June 2018: Supercell on the Kansas-Oklahoma border

The UMass LPR crew intercepted a long-lived, high-precipitation (HP) supercell on the Kansas-Nebraska border on the evening of 12 June 2018. Owing to persistent back-building toward the southwest along the dryline, its mean storm motion was toward the west-southwest. Four deployments were attempted, with the longest and most successful occurring near Rosston, Oklahoma from 2335 UTC on 12 June to 0107 UTC on 13 June 2018. Several transient low-level circulations, some anticyclonic, were noted along the leading edge of the hook echo around 1 km AGL (e.g., Fig. 5). However, at lower tilts, the storm was strongly outflow-dominated (not shown), and no tornadoes were reported with this storm. The UMass LPR undeployed when the supercell, which contained large hail, approached the radar site. We categorize this case as one of tornadogenesis failure.

As with the Burwell, Nebraska data, we visualized the  $Z_{DR}$  column of the Rosston supercell in three dimensions by objectively analyzing the  $Z_{DR}$  field to a 200-m grid (Fig. 6). Again, it appears that UMass LPR did not sample the  $Z_{DR}$  column of the Rosston supercell through its full depth, as it is evident that even the highest elevation scan intercepted the  $Z_{DR}$  column's interior. As the column's range decreased from 15 to 7 km north of the UMass LPR deployment site the  $Z_{DR}$  column top height coincided with the height of the 30° beam in all but the first few scans, (Fig. 7). This finding reinforces the notion that UMass LPR needs to be deployed at slightly longer ranges (15-25 km) from target storms.

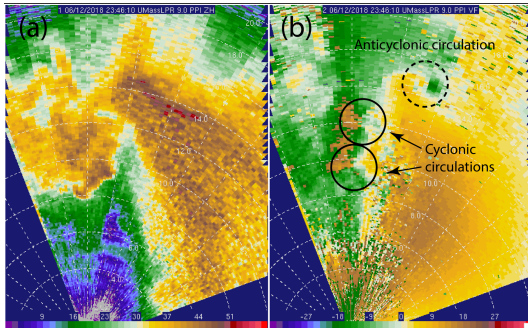


Fig. 5. As in Fig. 3, but in the hook of the Rosston, Oklahoma HP supercell at 2348 UTC on 12 June 2018 at an elevation angle of 9°. Two cyclonic circulations (solid black circles) and one anticyclonic circulation (dashed black circle) are annotated.

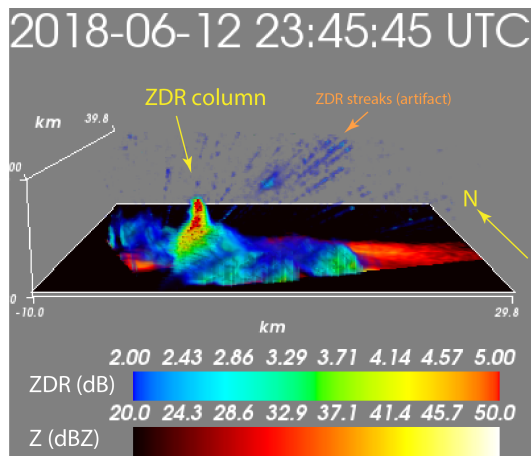


Fig. 6. As in Fig. 4, but for the Rosston, OK storm of 12 June 2018 at 2346 UTC. The view is toward the north. The scalloped / amphitheater-like appearance of the  $Z_{DR}$  column's interior surface results from the objective analysis of the highest elevation scan (30°), which intersects the column, onto the 200-m grid. The features denoted "ZDR streaks" are *not* depolarization streaks (e.g., Kumjian 2013), as the UMass LPR uses an ATAR polarization scheme.

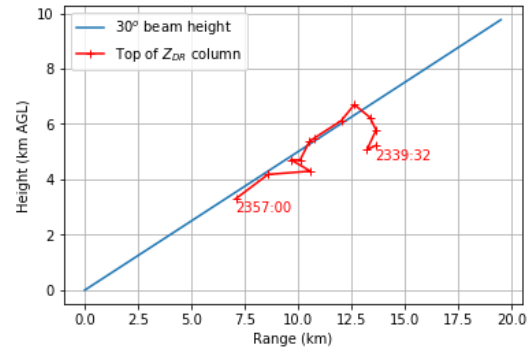


Fig. 7.  $Z_{DR}$  column top height in the Rosston storm as a function of range from UMass LPR from 2339 to 2357 UTC on 12 June 2018. The height of the 30° beam as a function of range (assuming standard atmospheric refraction) is plotted in blue.

#### 4. Conclusions

A DP PAR with a 1.9° azimuthal beam width was deployed near several severe storms in the spring of 2018. Two tornadogenesis failure cases were documented (Table 2). Observations of  $Z_{DR}$  columns were collected with approximately 90-s temporal resolution, at elevation angles up to 30°. Even though these volumes are deep when compared with those collected by a WSR-88D in precipitation mode (19.5°), it was determined that in order to sample the full depth of a  $Z_{DR}$  column that is 8 km in height (Snyder et al. 2015) the UMass LPR must be deployed at a range of 15 to 25 km from the target storm. Another option is to tilt the antenna array back a few degrees, shifting the elevation sector upward and sacrificing the lowest elevation scans.

Some data quality issues with the UMass LPR observations still remain to be addressed and are described elsewhere in this session (Heberling et al. 2019). Chief among these is the fact that UMass LPR had no leveling system available in 2018. However, the pitch, roll, and heading of the UMass LPR truck were recorded at every deployment to an accuracy of  $\pm 0.2^\circ$  by an onboard compass and GPS system. It may be possible to partially correct for imperfect leveling of the truck in postprocessing.

UMass LPR will be used again in Spring 2019 to collect additional  $Z_{DR}$  column observations in supercells. Contemporaneous efforts are underway to catalog and analyze RS DP observations of supercells from previous field campaigns (Dalman et al. 2018).

## Acknowledgments

Field work and data analysis were supported by NSF grant AGS-1741003 to the first author. Mobilization and testing of the UMass LPR was supported by National Science Foundation (NSF) grant AGS-1655693 to the fourth author. Dr. Darryl Granger (EAPS department head) generously sponsored travel for the Severe Storms Field Work course in 2018. We also gratefully acknowledge the eight student participants who assisted with this years' field deployments. Radar plots were generated using Solo II (<https://rose.eol.ucar.edu/>), Mayavi (Ramachandran and Varoquaux 2011), and Py-ART (Helmus and Collis 2016).

## References

- Bluestein, H. B., J. C. Snyder, and J. B. Houser, 2015: A multi-scale overview of the El Reno, Oklahoma, tornadic supercell of 31 May 2013. *Wea. Forecasting*, **30**, 525-552, doi:10.1175/WAF-D-14-00152.1.
- Bluestein, H. B., R. M. Rauber, D. W. Burgess, B. Albrecht, S. M. Ellis, Y. P. Richardson, D. P. Jorgensen, S. J. Frasier, P. Chilson, R. D. Palmer, S. E. Yuter, W.-C. Lee, D. C. Dowell, P. L. Smith, P. M. Markowski, K. Friedrich, and T. M. Weckwerth, 2014: Radar in atmospheric sciences and related research: Current systems, emerging technology, and future needs. *Bull. Amer. Meteor. Soc.*, **95**, 1850-1861, doi:10.1175/bams-d-13-00079.1.
- Crowe, C. C., C. J. Schultz, M. R. Kumjian, L. D. Carey, and W. A. Petersen, 2012: Use of dual-polarization signatures in diagnosing tornadic potential. *Electronic J. Operational Meteor.*, **13**, 57-78,
- Dalman, D. M., R. L. Tanamachi, P. E. Saunders, B. L. Cheong, D. Bodine, H. B. Bluestein, and Z. B. Wienhoff, 2018: Cataloging rapid scan observations of ZDR columns in supercells. *29th Conf. on Severe Local Storms*, Stowe, Vermont, American Meteorological Society, P89, <https://ams.confex.com/ams/29SLS/webprogram/Paper348610.html>.
- Dawson, D. T., J. Bozell, J. Buckingham, W. L. Downing, D. R. Chavas, H. M. Mallison, M. I. Biggerstaff, and S. Waugh, 2016: Overview of Purdue's mobile disdrometer observations during VORTEX-SE. *28th Conf. on Severe Local Storms*, Portland, Oregon, American Meteorological Society, 16A.12,
- <https://ams.confex.com/ams/28SLS/webprogram/Paper301887.html>.
- French, M. M., H. B. Bluestein, I. PopStefanija, C. A. Baldi, and R. T. Bluth, 2014: Mobile, phased-array, Doppler radar observations of tornadoes at X-band. *Mon. Wea. Rev.*, **142**, 1010-1036, doi:10.1175/mwr-d-13-00101.1.
- Heberling, W., J. Waldinger, and S. J. Frasier, 2017: An X-band phased array weather radar testbed. *38th Conf. on Radar Meteorology*, Chicago, Illinois, American Meteorological Society, P123, <https://ams.confex.com/ams/38RADAR/webprogram/Paper320970.html>.
- Heberling, W., S. J. Frasier, C. Wolsieffer, and M. Adams, 2019: X-Band Phased-Array Weather-Radar Polarimetry Testbed: Bias Expectation and Preliminary Results. *Phased Array Radar Symp., 99th American Meteorological Society Annual Meeting*, Phoenix, Arizona, American Meteorological Society, 1.2, <https://ams.confex.com/ams/2019Annual/meetingapp.cgi/Paper/350300>.
- Heinselman, P., D. LaDue, D. M. Kingfield, and R. Hoffman, 2015: Tornado warning decisions using phased array radar data. *Wea. Forecasting*, **30**, 57-78, doi:10.1175/WAF-D-14-00042.1.
- Heinselman, P. L., D. L. Priegnitz, K. L. Manross, T. M. Smith, and R. W. Adams, 2008: Rapid sampling of severe storms by the National Weather Radar Testbed Phased Array Radar. *Wea. Forecasting*, **23**, 808-824, doi:10.1175/2008waf2007071.1.
- Helmus, J. J., and S. Collis, 2016: The Python ARM Radar Toolkit (Py-ART), a library for working with weather radar data in the Python programming language. *Journal of Open Research Software*, **4**, e25, doi:10.5334/jors.119.
- Houser, J. B., H. B. Bluestein, and J. C. Snyder, 2015: Rapid-scan, polarimetric, Doppler-radar observations of tornadogenesis and tornado dissipation in a tornadic supercell: The "El Reno, Oklahoma" storm of 24 May 2011. *Mon. Wea. Rev.*, **143**, 2685-2710, doi:10.1175/MWR-D-14-00253.1.
- Houser, J. L., H. B. Bluestein, and J. C. Snyder, 2016: A finescale radar examination of the tornadic debris signature and weak-echo reflectivity band associated with a large, violent tornado. *Mon. Wea. Rev.*, **144**, 4101-4130, doi:10.1175/MWR-D-15-0408.1.

- Kumjian, M. R., 2013: Principles and applications of dual-polarization weather radar. Part III: Artifacts. *J. Operational Meteor.*, **1**, 265–274, doi:<http://dx.doi.org/10.15191/nwajom.2013.0121>.
- Kurdzo, J. M., F. Nai, D. J. Bodine, T. A. Bonin, R. D. Palmer, B. L. Cheong, J. Lujan, A. Mahre, and A. D. Byrd, 2016: Observations of severe local storms and tornadoes with the Atmospheric Imaging Radar. *Bull. Amer. Meteor. Soc.*, **98**, 915-935, doi:10.1175/BAMS-D-15-00266.1.
- Orzel, K. A., 2015: X-band dual polarization phased-array radar for meteorological applications. Dissertation, Electrical and Computer Engineering, University of Massachusetts Amherst, 165 pp.
- Pazmany, A. L., J. B. Mead, H. B. Bluestein, J. C. Snyder, and J. B. Houser, 2013: A mobile, rapid-scanning, X-band, polarimetric, (RaXPoL) Doppler-radar system. *J. Atmos. Oceanic Technol.*, **30**, 1398–1413, doi:10.1175/jtech-d-12-00166.1.
- Picca, J. C., J. C. Snyder, and A. V. Ryzhkov, 2015: An observational analysis of ZDR column trends in tornadic supercells. *37th Conf. on Radar Meteorology*, Boston, Massachusetts, American Meteorological Society, 5A.5, <https://ams.confex.com/ams/37RADAR/webprogram/Paper275416.html>.
- Puzella, A., and R. Alm, 2007: Air-Cooled, Active Transmit/Receive Panel Array. *2007 IEEE Radar Conference*, 421-426, doi:10.1109/RADAR.2007.374253,
- Ramachandran, P., and G. Varoquaux, 2011: Mayavi: 3D Visualization of Scientific Data. *IEEE Computing in Science & Engineering*, **13**, 40-51, doi:10.1109/MCSE.2011.35.
- Salazar-Cerreño, J. L., T.-Y. Yu, C. Fulton, M. McCord, R. D. Palmer, H. B. Bluestein, B. L. Cheong, M. I. Biggerstaff, B. M. Isom, J. M. Kurdzo, J. R. Doviak, X. Wang, and M. Yeary, 2017: Development of a mobile C-band Polarimetric Atmospheric Imaging Radar (PAIR). *97th American Meteorological Society Annual Meeting, Special Symposium on Meteorological Observations and Instrumentation*, Seattle, Washington, American Meteorological Society, 1B.1, <https://ams.confex.com/ams/97Annual/webprogram/Paper308655.html>.
- Snyder, J. C., A. V. Ryzhkov, M. R. Kumjian, and J. Picca, 2015: A ZDR column detection algorithm to examine convective storm updrafts. *Wea. Forecasting*, **30**, 1819-1844, doi:<http://dx.doi.org/10.1175/WAF-D-15-0068.1>.
- Stailey, J. E., and K. D. Hondl, 2016: Multifunction Phased Array Radar for Aircraft and Weather Surveillance. *Proc. IEEE*, **104**, 649-659, doi:10.1109/JPROC.2015.2491179.
- Tanamachi, R. L., D. T. Dawson II, and L. Carleton Parker, 2019: Students of Purdue Observing Tornadic Thunderstorms for Research (SPOTTR): An update. *28th Symp. on Education*, Phoenix, Arizona, American Meteorological Society, 8.2, <https://ams.confex.com/ams/2019Annual/meetingapp.cgi/Paper/350955>.
- Tanamachi, R. L., H. B. Bluestein, J. B. Houser, K. M. Hardwick, and S. J. Frasier, 2012: Mobile, X-band, polarimetric Doppler radar observations of the 4 May 2007 Greensburg, Kansas tornadic supercell. *Mon. Wea. Rev.*, **140**, 2103-2125, doi:10.1175/MWR-D-11-00142.1.
- Wurman, J., K. Kosiba, P. Robinson, and T. Marshall, 2014: The role of multiple vortex tornado structure in causing storm researcher fatalities. *Bull. Amer. Meteor. Soc.*, **95**, 31-45, doi:10.1175/bams-d-13-00221.1.
- Zhang, G., R. J. Doviak, D. S. Zrnić, R. Palmer, L. Lei, and Y. Al-Rashid, 2010: Polarimetric phased-array radar for weather measurement: A planar or cylindrical configuration? *J. Atmos. Oceanic Technol.*, **28**, 63-73, doi:10.1175/2010JTECHA1470.1.